Clim. Past Discuss., 10, 977–1023, 2014
www.clim-past-discuss.net/10/977/2014/
doi:10.5194/cpd-10-977-2014

Climate of the Past
Discussions
Open Access

46 000 years of alternating wet and dry phases on decadal to orbital timescales in the cradle of modern humans: the Chew Bahir project, southern Ethiopia

V. Foerster[1], A. Junginger[2], A. Asrat[3], H. F. Lamb[4], M. Weber[5], J. Rethemeyer[5], U. Frank[6], M. C. Brown[6], M. H. Trauth[2], and F. Schaebitz[1]

[1]University of Cologne, Seminar for Geography and Education, Gronewaldstrasse 2, 50931 Cologne, Germany
[2]University of Potsdam, Institute of Earth and Environmental Science, Germany
[3]Addis Ababa University, Department of Earth Sciences, P.O. Box 1176, Addis Ababa, Ethiopia
[4]Aberystwyth University, Department of Geography and Earth Sciences, Aberystwyth SY23 3DB, UK
[5]University of Cologne, Institute of Geology and Mineralogy, Zülpicher Str. 49A, 50674 Cologne, Germany
[6]Helmholtz-Zentrum Potsdam, Deutsches GeoForschungsZentrum – GFZ, 14473 Potsdam, Germany

Received: 9 January 2014 – Accepted: 20 January 2014 – Published: 7 March 2014

Correspondence to: V. Foerster (v.foerster@uni-koeln.de)

Published by Copernicus Publications on behalf of the European Geosciences Union.

Abstract

Rapid changes in environmental conditions are considered to be an important driver for human evolution, cultural and technological innovation, and expansion out of Africa. However, the nature of these environmental changes, their amplitude and correlation with steps in human evolution is the subject of current debates. Here we present a high-resolution (~3–12 yr) and well-dated (32 AMS ^{14}C ages) lake-sediment record of the last 46 000 yr from the Chew Bahir basin in the southern Ethiopian Rift. The record was obtained from six cores along a NW–SE transect across the basin, which has been selected as the drilling location within the ICDP Hominin Sites and Paleolakes Drilling Project (HSPDP). Multi-proxy data and the comparison between the transect coring sites provide initial insight into intra-basin dynamics and major mechanisms controlling the sedimentation of the proxies that was used to develop a basic proxy concept for Chew Bahir for the last two wet-dry cycles. The environmental response to orbitally induced sinusoidal insolation changes is usually nonlinear, as climate changes abruptly compared to changes in the forcing, or gradual but punctuated by multi-decadal intervals of drier conditions. The second major control on the environment is millennial-scale climate variability lasting ~1500 yr, similar in duration to the high-latitude Dansgaard–Oeschger cycles and Heinrich events including the Younger Dryas cold reversal at the end of the last glacial, mostly causing abrupt shifts from extreme arid to wet conditions. The duration and character of orbitally induced, high-latitude controlled, and multi-decadal climate shifts provides important constraints for the adaptation of humans to the changing environment. Therefore, Chew Bahir is a perfect site to study and understand climatic variability on different timescales.

1 Introduction

The *cradle of humankind* is today widely agreed to be located in the climatically and topographically diverse East African Rift System (EARS) that provided a highly variable environment to enable and push the evolution of mammals (Tishkoff and Verrelli, 2003;

Trauth et al., 2010). The oldest known fossil remains of anatomically modern humans (AMH), dated to 195 ka BP were found in the Omo Region in the southwestern part of Ethiopia (White et al., 2003; McDougall et al., 2005). From here, modern humans dispersed into Asia and Europe to eventually populate the world (Stringer et al., 2003; Oppenheimer, 2009).

Determining the nature, character, and pace of a changing environment of early humans is crucial to understanding the factors that influenced human evolution (Vrba, 1985; Potts et al., 1998; Maslin and Trauth, 2009) and dispersal, including cultural and technological innovations (Hildebrand and Grillo, 2012; Vogelsang and Keding, 2013). The timing and synchronicity of the dry-wet cycles that have significantly modulated the East African climate is of particular interest, as they would also have had important implications for human adaptation and survival in refugia (Ambrose et al., 1998; Hildebrand et al., 2010) or might have pushed the dispersal beyond Africa during major droughts (Carto et al., 2009) or enabled migration along possible green corridors (Castañeda et al., 2009).

However, understanding the complex mechanisms driving climate shifts is a challenging task considering the uncertainties in reconstruction and attribution to the possible driving mechanisms. Numerous recent studies (e.g. Mulitza et al., 2008; Verschuren et al., 2000; Tierney et al., 2011; Junginger and Trauth, 2013) show that the system is far more complex than assumed years ago. For instance, the timing and abruptness of the transition and internal variability of the youngest and therefore best-studied dry-wet cycle, the so-called African Humid Period (AHP, 15–5 ka BP) has been debated for decades (e.g. deMenocal et al., 2000; Kröpelin et al., 2008; Tierney and deMenocal, 2013; Junginger et al., 2014). For Lake Turkana alone more than three different possible terminations of the AHP have been reconstructed (Johnson et al., 1991; Brown and Fuller, 2008; Garcin et al., 2012). Generally, issues include the non-continuity of records where gaps in the record during dry phases hamper the understanding of the climatic history, dating uncertainties, site or proxy-specific responses to climate change or comparing marine and terrestrial archives.

Thus, the area, what is southern Ethiopia and northern Kenya today, possibly representing the source region of modern humans, is naturally an ideal place to study the close interplay of humans and climate (Cohen et al., 2009). This paper presents a contribution towards understanding the climatic dynamics of the source region of modern man, given the proximity (Fig. 1) to the paleoanthropological site of the Omo-Kibish, from the 46 000 yr record contained in a transect of cores through the Chew Bahir basin in southern Ethiopia. The study presented here is an approach to show the climatic history covering the last two orbitally driven dry-wet cycles while taking proxy and site specificity of signals as well as dynamics within the basin itself into account. These results constitute preliminary data for the Hominin Sites and Paleolake Drilling Project (HSPDP; Cohen et al., 2009) that tackles exactly this issue of understanding the paleoclimatic context of human evolution through scientific drilling.

2 Regional setting

2.1 Geology and geomorphology

Chew Bahir (4.1–6.3° N; 36.5–38.1° E), today a 30 km × 70 km saline mudflat in a tectonically bounded basin in southern Ethiopia is situated in a biogeographically highly sensitive transition zone between the southern sector of the Main Ethiopian Rift (MER) to the northeast and the Omo-Turkana basin to the west (Fig. 1a). This ∼250 km wide broadly rifted zone (BRZ, Ebinger et al., 2000; WoldeGabriel and Aronson, 1987) is characterised by small fault bounded depressions, providing an archive for sedimentary deposits beyond the Quaternary as the basin and range landscape was formed during older phases of the rifting process (Ebinger et al., 2000; Corti, 2009). The sediments (Fig. 1b) in the catchment comprise lacustrine silt and clay, fluvial silt and sand, and alluvium. The Chew Bahir basin is bounded by the Hammar range to the west, composed of Precambrian basement, mainly undivided gneisses, and the higher escarpment of the Teltele Plateau, exposing Miocene basalts and trachytic centres to

the East (Fig. 1b). Its northern sector is formed by the narrower Weyto basin bounded by the southwestern (Gofa) highlands to the west and the Gamo-Chencha horst to the east. In the northern, northwestern and northeastern part of the catchment Oligocene basalt flows with subordinate rhyolite, trachyte, tuffs and ignimbrites are the dominant lithology. To the south, the Chew Bahir basin extends to the broadly rifted zone that lies between the Ethiopian and Kenyan uplifted domes (WoldeGabriel and Aronson, 1987; Pik, 2008; Corti, 2009). The perennial rivers Weyto and Segen wash in deposits from the ∼32 400 km^2 catchment, though their influence today is limited to the northern part of the basin by forming a delta further into the basin (Fig. 1e) (Foerster et al., 2012). Today the basin is merely episodically covered by a few centimetres of water immediately after the rainy season, mostly due to an overflow of the Weyto into the basin. In addition, Chew Bahir receives deposits via the extensive alluvial fans off the escarpment flanks: the Hammar Range to the west and the Teltele Plateau to the east. However, the small drainage networks at the border faults and the strong seasonality in rainfall make this sediment and water influx highly episodic, because the runoff is closely connected to strong rainfall events during the two rainy seasons and occasional orographic rains. During humid phases Chew Bahir represented the southernmost end point of the drainage system of the Ethiopian Rift Lakes (Junginger and Trauth, 2013; Junginger et al., 2014), and is known to have an overflow level ∼50 m above the present basin floor into Lake Turkana (Fig. 1b; Foerster et al., 2012). The basin has sensitively reacted in the past to the drastic moisture fluctuations with a variable lake filling: from an extensive fresh water lake to a saline mudflat.

2.2 Present climate

East Africa's climate is governed by moisture availability driven by strong rainfall seasonality, closely tied to the annual latitudinal migration of the Intertropical Convergence Zone (ITCZ) between 15° N in July and 15° S in January. The ITCZ follows maximum insolation values of the overhead sun with a four to six week time lag (Nicholson, 1996) (Fig. 1), and thus, creates a largely zonal rainfall pattern. The

seasonal migration of the ITCZ attracts moisture through large-scale advection from the Indian Ocean (Levin et al., 2009) resulting in a bimodal annual climatic cycle, with "long rains" from March to May and "short rains" in October–November in the equator regions and only one rainy season at the northern and southern migration margins (Nicholson, 1996). The south-westerly humid Congo air stream delivers additional rainfall to the western parts of equatorial East Africa and Northwestern Ethiopia roughly between July and September, when the ITCZ has reached its northernmost position (known as the "September rains" in some areas of Kenya and "Kiremt" in Ethiopia; Nicholson, 1996; Camberlin, 1997; Segele and Lamb, 2005). Moisture delivered by the Congo air stream is sourced from the Atlantic Ocean and associated with the West African summer Monsoon (WAM). It is in part recycled from vegetation to the atmosphere during its transit across the Congo basin (Nicholson, 1996). This unstable flow from the Atlantic converges with drier air masses from the Indian Ocean along a north-south trending zone known as the Congo Air Boundary (CAB). Due to diverse topography of EARS and the relative position to the equator, temperatures vary only slightly, merely across elevation gradients. Various microclimates (Fig. 1) with a pronounced evaporation/precipitation gradient are thus created also for the Chew Bahir catchment with generally cooler highlands receiving most rainfall that runs off into the hotter and drier lowlands (Gasse et al., 2000; Seleshi and Zanke, 2004). Figure 1 demonstrates that even adjacent to the catchment of Chew Bahir rainfall is highly dependent on elevation and position towards the influence of ITCZ and Congo Air Boundary (CAB).

3 Material and methods

3.1 Field campaign

Five short cores (CB-02–CB-06) of 9–11 m in length were retrieved with a percussion corer in November 2010 along a NW–SE transect through the now desiccated floor of the Chew Bahir basin (Table 1 and Fig. 1b, d and e). Supplemented by the 18.86 m long

pilot core CB-01 drilled in 2009 (Foerster et al., 2012), the six cores cover a marginal area from extensive alluvial fans off the Hammar range in the west (CB-01 and CB-02), and eastwards through an intermediate area influenced by fluvial, lacustrine and alluvial fan run-off (CB-03) towards the centre of the basin (CB-05, CB-06, CB-04). Coring at each site was continuous without overlap. Each drive measured 100 cm, controlled by the equivalent length of the drilling rods. 1 m plastic liners with an inside diameter of 4.8 cm were used to retain the core sections. Core catcher material was analysed in the field for material composition, grain size and colour. The overall core recovery ranges from 97 to 99.5 %, with minor core loss due to unconsolidated material at the top (Fig. 3). The cores were directly sealed at the site and shipped by airfreight to the University of Cologne, where they were stored in a cool and dark place before further analysis.

3.2 Core composition of CB-03 and CB-05

The total length of the CB-03 (Fig. 3a) profile is 11.0 m and comprises 10.8 m of sediment due to coring without a replicate and a 98 % recovery rate (Table 1). No gaps occur, the only core loss being of the uppermost section, which has been subjected to soil formation and was in a rather unconsolidated form (0–20 cm). CB-05 (Fig. 3b) covers the uppermost 10 m of the deposits, comprising 9.62 m of sediment, as CB-05 is interrupted by one gap at 4.00–4.08 m, supposedly caused by high water content when coring through the groundwater level and 30 cm core loss from the soil horizon at the top of the core. Hiati in the records cannot be excluded but are not obvious. The composition of the cores is uniform, consisting of lacustrine silts and clays, intercalated by layers of coarse-grained silts and sands and evaporitic carbonate layers (Fig. 3a and b). In addition to this general composition, we found several thick layers with fish bones, some horizons rich in molluscs, and several units that show a matrix of fine clays partly disturbed by distinctive tooth shaped illuvations (Fig. 3a and b).

For the comparative approach of this study we restricted our analysis to CB-05 as representative core for the central area as it provides the most continuous record

back to +46 ka BP and CB-03 from the intermediate basin area, while CB-03 provides ~3 yr resolution during the AHP. We interpret those cores together with the previously described pilot core CB-01 (Foerster et al., 2012) from the western margin of the basin.

3.3 Sedimentology and geochemistry

All core sections were split lengthwise with a manual core splitter, then described, scanned and later subsampled at 1–2 cm intervals largely following the established principles of Ohlendorf et al. (2011). Samples were freeze-dried to guarantee adequate storage of the samples to preserve them for future analysis and facilitate fine grinding without compromising the mineral structure. Smear slides were prepared in ~30 cm intervals to provide a first insight into the composition, microfossil occurrences (diatoms, pollen, charcoal), volcanic glasses and accomplish scanning results so that sections with prioritised interest could be identified for further analysis.

Elemental composition of the cores was determined at 500 µm resolution with an Itrax X-ray fluorescence (XRF) core scanner (Cox Analytical Systems) using a Chromium (Cr) tube as radiation source, a tube voltage of 30 kV, a current of 30 mA and, an exposure time of 20 s. As argued already in Foerster et al. (2012), the common practise of using element ratios (e.g. Croudace et al., 2006) was not applied stringently, in order to avoiding the mixing of different processes behind elemental composition. For comparison with the pilot core, which was measured with a Mo tube, all records were standardised (mean = 0, standard = 1).

Grain sizes were estimated semi-quantitatively by finger test, with the sediment composition subdivided into 7 fractions (clay = 1 to sandy gravel = 7; Fig. 3). XRD analysis with a Siemens D5000 diffractometer was applied to finely ground bulk samples from all cores. No further treatment or the addition of a standard indicator was necessary for using this semi-quantitative approach. EVA (DIFFRAC-AT) was used for phase identification. Total nitrogen (TN), total carbon (TC), and total organic carbon (TOC) contents were determined, but with distinctly low organic content ranging around

0.2 wt%, values were in general too low to be used as an environmental parameter and thus will be excluded from further discussion (Meyers, 2003).

After diatom assemblages were outlined by smear slide analyses, samples at 2–10 cm resolution were treated with hydrogen peroxide (H_2O_2, 30 %) and hydrochloric acid (HCl, 37 %) to remove remaining organic components and the fine sticky clays from the diatom frustules and to dissolve carbonates, respectively. After thorough washing and adding microspheres to the solution, the diatom suspension was mounted on microscope slides and fixed with Naphrax for an optimised light refraction. A light microscope complemented with a polarizer and REM pictures were used for taxa identification.

3.4 Rock magnetic measurements and core correlation

Rock magnetic and high resolution susceptibility measurements on the Chew Bahir transect cores were carried out at the Helmholtz Center Potsdam – Deutsches GeoForschungsZentrum GFZ (Frank et al., 2011; Brown et al., 2012). Remanence measurements (NRM, ARM, IRM, S-ratio, HIRM) and susceptibility were used in combination with the XRF records and MSCL analyses to find the most reliable proxy set to correlate the transect cores. Eventually, the potassium record (depth) of cores CB03-06 has been tuned to the potassium record of the master core CB01 assuming that K, as a weathering product of feldspar, feldsparthoids and mica, is transported instantaneously in solution from source to sink, and complete mixing in the water body of paleo-lake Chew Bahir. We restricted the choice of tie points to < 15 critical turning points and distinct peaks to restrict the error of prediction (Figs. 5 and 6). The distinct event markers in the Ca record and anti-correlated trends in the Cl record were used to provide cross control.

3.5 Chronology

Age control is principally provided by 32 AMS ^{14}C ages derived from biogenic carbonates (mostly the common gastropod *Melanoides tuberculata*), organic sediment, and detrital charcoal (Table 2, Fig. 2). Our best estimate of age was obtained by calculating the weighted mean of the probability density function (PDF) of each age. To get the PDF we used OxCal (Bronk Ramsey, 1995) with 1-sigma error and converted radiocarbon dates to calendar years taking all probabilities into account. Ages shown in the age-depth model in Fig. 2 correspond to the weighted means out of this PDF. Additionally, we present radiocarbon ages in Table 2 with a 2-sigma error and the 2-sigma interval of ages calibrated using the IntCal09 data set (Reimer et al., 2009) within the CALIB 6.0html calibration programme (Stuiver et al., 2005) to demonstrate the maximal possible probability interval induced by the calibration. Furthermore this demonstrates that some of the outlier ages cannot be attributed to the calibration process or even the calibration programme that was used. For several dates calibration resulted in multiple possible age ranges with differing probabilities (Table 2).

No age control for the surface is available, but since large parts of the basin were covered by water until the late 60's of the last century and the inclination of the basin slopes is almost even, we anticipate that large-scale erosion in the recent past can be excluded. We thus assume an age of 1960 AD for the surface of the Chew Bahir basin.

To assess a possible reservoir effect on the dated carbonates we scanned CB-03 in 20 cm intervals for sufficient charcoal particles (as terrestrial plant remains; Geyh et al., 1998) and/or shell fragments from the same horizons. The paired dating approach was not successful as charcoal is almost absent throughout the cores. Only at 204 cm depth in CB-03 was just enough material found for parallel dating of shell fragments and charcoal. Parallel bulk/shell sampling was also used as an alternative approach to determine a possible reservoir effect in the carbonate material.

4 Results and proxy evaluation

4.1 Age model and core chronology

The composite age-depth model (Fig. 2) is based on 32 calibrated AMS ^{14}C dates (Table 2), including six ages from the published pilot core CB01. A closer look at the age model reveals a number of outliers that are either too young or too old to fit the estimated age and to be in line with the other age determinations. As described in great detail by others (Björck and Wohlfarth, 2001; Cohen et al., 2003; Felton et al., 2007; Kliem et al., 2013) there may be several explanations. For deviations on smaller timescales (up to a few centuries), a reservoir effect (old carbon effect) or a plateau effect in calibration could be taken into consideration. Much larger offsets however, can be caused by remobilisation of dated material prior to deposition, redistribution within the basin, stratigraphical mixing caused by bioturbation, infills of dry cracks, or sample contamination with modern carbon during coring or later in the lab.

The Chew Bahir ages have not been corrected for a possible reservoir effect, where ages derived from biogenic carbonates would be slightly older if they had been compromised by fossil carbon as in many archives (e.g. Felton et al., 2007; Kröpelin et al., 2008; SOM; Junginger et al., 2014). However, this seems not the case for the Chew Bahir samples, though a reservoir effect could be neither determined nor ruled out as there were too few pair dated samples (charcoal and carbonates) and those few we could pair date are all clear outliers. The three most prominent anomalously young dates from CB-03 (Beta 329853, Beta 329854 parallel dating at 389 cm composite depth and Beta 329855 at 743 cm composite depth in Fig. 2) have most likely entered the record via ground water circulation. Given the extreme scarcity of picked particles in the sample and rather small particle size, the dated material is extremely mobile. The few other closely together dated samples (organic bulk and carbonates) do however not suggest a tendency towards carbonates being consistently older compared to organic samples as Fig. 2b shows. Whereas the dated carbonates (COL 1235) from the reworked section in CB-05 are significantly older then the organic

sediment sample COL1632 from the same horizon, the pair dated samples from CB-03 show the opposite tendency, with the mollusc being younger than the bulk material.

Following, the ages that are not in line with the reliable age determinations are attributed to possible reasons that might have caused the offset, from bottom to top of the composite depth of the age model in Fig. 2.

COL 1631 from CB-05 (1890 cm composite depth in Fig. 2) is very likely to have been compromised by modern carbon after coring and shows the maximal offset of ~20 ka. The two apparently anomalously young Holocene ages from CB-05 (COL1632 and COL1830) at 617 and 711 cm composite depth may have been subject to reworking or stratigraphical mixing during the AHP lake phase as suggested by the rather noisy proxy records and sedimentological structure in parts of the Holocene deposits of CB-05 that indicate that the material has been heavily reworked. A series of radiocarbon ages derived from organic sediment between 650 and 300 cm composite depth are slightly but consistently too old. These three ages from CB-01 (Beta 347311–347313) and five ages from CB-03 (Beta 347314–347318) are slightly offset by ~100 cm compared with the African Humid Period (15–5 ka, ~750–400 cm composite depth) suggesting temporary storage and remobilisation of organic matter in the densely vegetated catchment during a wetter climate (Fig. 2b). Several ages, all derived from the distinct gastropod horizon (see also Sect. 4.5) deposited briefly after the YD, show a temporal offset (< 500 yr) towards being slightly too old (COL 1228, 1231, 1630, 1235, 1832; note the several too old mollusc ages with green symbols around 11–12 ka BP in Fig. 2). These five ages though, are dated to a time interval within the termination phase of the YD when a shallow lake (< 10 m) provided a suitable habitat for *M. tuberculata*. Assuming however, that the radiocarbon dates themselves are reliable, redeposition within a rapidly re-establishing lake as cause for the offset seems most likely. Therefore we treat all ages from this layer as a reliable biological age control point, strongly supporting our correlation, but have to refrain from including them in the age model as the original depth cannot be attributed due to redeposition.

The most reliable age model for our ages from the Chew Bahir records is a conservative composite age-depth model using a linear interpolation technique. We prefer a linear over a spline model as abrupt variations between low or high sedimentation rates, even episodes without deposition, may actually exist in rift environments, but are smoothed out by splines and age modelling techniques introducing an arbitrary chosen memory (e.g., Bronk Ramsey, 2008, 2009; Blaauw and Christen, 2011; Trauth, 2014). However, we used linear and cubic spline interpolation techniques while tuning the individual records but we have found no significant difference in the final result. Finally, the CB proxy records were interpolated upon the composite age model, also using a linear interpolation technique.

The composite age-depth model shows a two-time change in the sedimentation rate (Fig. 2). The changes in the sedimentation rates are governed by the dry-wet variations, as higher sedimentation is coinciding with wet phases, whereas aridity is expressed in significantly lower sedimentation per year. The composite age model shows clearly that two wet episodes with five to six-fold sedimentation rates bracket an episode of a drier climate during the last glacial maximum with sedimentation rates of ~0.1 mm yr^{-1}. The sedimentation rates vary not only through time, but also within the basin from the shore to the paleo-lake center: the highest mean sedimentation rate was identified for the pilot core (CB-01) at the margin of the basin with ~0.7 mm yr^{-1}, whereas for CB-05, 16.2 km southeast into the center of the mudflat, we deduct a mean of ~0.2 mm yr^{-1}. Intermediate values apply for CB-03 with ~0.4 mm yr^{-1}. There is therefore a clear decrease of sedimentation rate towards the basin centre, which naturally affects the duration and resolution of the records. Extrapolating the sedimentation rate linearly, CB-03 has a maximum age of ~26.5 ka cal BP at 11 m depth. CB-05 covers a maximum of ~46 of sediment history in 10 m sediment depth.

According to the core chronology, the sedimentary records span climate history from ~46 to ~300 yr BP and thus cover the expression of global climate events in southern Ethiopia, including the timing and character of the Last Glacial Maximum (LGM, 23–18 ka BP), the African Humid Period (AHP, 15–5 ka), the Younger and the Older Dryas

(YD, 12.8–11.6 ka BP and OD, around 14 ka BP) and towards the top of the records the Medieval warm period (MWP, 700–1000 BP).

4.2 Physical parameters and mineralogy

The magnetic susceptibility (MS) logs show a distinct signature that probably could indicate rather large climate transitions than small scale changes as a correlation between grain sizes is not significant amongst the cores. Grain-size variations show a correlation between coarser material and drier intervals especially towards the onset of arid conditions. The products of prevailing physical weathering during aridity may have been transported into the basin in highly episodic but strong rainfall events. Furthermore, up to 5 mm big Ca-rich precipitates occur during dry intervals that were probably formed during intervals with strongly increased evaporation.

The qualitative XRD measurements on selected samples show the overall composition of the material and changes in the mineral assemblages of different sections (for full account of mineral assemblages and their attributed provenance see Foerster et al., 2012). The sediment contains calcite, analcime, sanidine, albite, anorthite, montmorillonite, muscovite, illite, quartz, epidote and orthoclase. There are variations in the proportions of members of the feldspar family and weathering products of volcanic materials, mainly basalts. The most characteristic sets are composed of analcime, calcite and montmorillonite or of orthoclase, quartz and illite. XRD results show that mineral assemblages vary significantly more along the core than across the core transect.

4.3 Chemical composition

The XRF scanning scans provided data on the elemental content of 26–47 elements, depending on the setting of the Itrax core scanner. Out of this, only the significant elements showing a clear paleoenvironmental signal were selected for further interpretation.

As Fig. 3a and b shows, the K records of CB-03 and CB-05 show distinct variations and trends throughout the record, punctuated by some noticeable markedly abrupt transitions, especially at 7.78 m in CB-03 (~15 ka; onset of the AHP) and 5.48 m in CB-03 (~11.8 ka; return to full humid conditions after YD). Furthermore, several short-term events expressed in sharp peaks in the K record modulate the long-term trends. K has previously been interpreted in core CB-01 as a reliable proxy for aridity, with increased input of K due to enhanced activity of the extensive alluvial fans off the slopes of the Hammar Range, when vegetation cover was reduced. The Hammar Range mainly composed of potassium-rich orthoclase feldspar-biotite-muscovite gneisses and two-mica granites, represents a restricted provenance, and during arid intervals, scarce strong rainfall events cause high input of these K-rich mineral particulates, while the continuous fluvial inwash into the basin decreases. As suggested by Burnett et al. (2011) and Govin et al. (2012), the prevailing mechanical weathering in more arid regions results in a characteristic abundance of illite and potassium feldspar, both being the most likely source of K. Furthermore, the dilution effect seems to be yet another major factor to drive a dramatic drop of K as soon as the big rivers draining into the CB basin become activated again with the onset of more evenly distributed and increased precipitation (Fig. 6).

The values for titanium (Ti), silica (Si) and partly iron (Fe) variations along the record are highly correlated (Fig. 3) with K, all reacting towards decreased moisture with higher values. They seem to be largely controlled by similar processes in the catchment and in the sediment, but are buffered, lagged or overprinted by other processes especially with a stabilising wet climate (lake phase). Besides a less constrained provenance of Ti, Si, and Fe we also suggest post-sedimentary diagenic redox processes overprinting the Fe signal, and autochthonous Si enrichments due to biogenic production such as diatom blooms.

The Chlorine (Cl) content is clearly anti-correlated to the elements named above responding with high values to wetter conditions (Figs. 3 and 6). Humidity proxy Cl reacts very sensitively with a sharp decrease to the onset of dry spells (Fig. 6). Cl has

a high solubility and reactivity, which makes it fast to react to humidity induced changes and sensitive to prevailing chemical weathering during humid phases. Shifts from physical to chemical weathering are clearly marked by sharp increases of Cl. However, the enhanced release of Cl during wet phases due to the intensification of chemical weathering in the whole catchment and the more or less continuous transportation of Cl into the basin by the big rivers also seems to predominate the dilution effect in a shallow lake.

Calcium (Ca) and the calcium-strontium ration (Ca / Sr) as a proxy to differentiate between biogenic carbonates (e.g. molluscs, ostracods, authigenc calcite) and allochthonous input are also largely anti-correlated to the first three elements. Though Ca and Ca / Sr do not show long-term trends, they serve as a distinctive marker proxy for the onset of humid conditions after enhanced dry phases (Fig. 3, e.g. in CB-03 at 5.20, 7.70 m and in CB-05 at 3.40 and 4.30 m; corresponding to the onset of wet conditions after the YD and the onset of the AHP respectively). It is presumed that calcite as a precipitate covers surface of the catchment area and is washed in in high abundance with the onset of wet conditions.

4.4 Fossil content

Freshwater diatoms, fish bones and some shells of the gastropod *Melanoides tuberculata* indicate lake episodes with fluctuating water levels throughout the whole record (Fig. 5). The gastropod *Melanoides tuberculata*, a very common and well-studied gastropod in African lakes, occurs as intact shells and shell fragments in several sections in all cores (see simplified column “fossil” in Fig. 3). This mollusc species is found in high abundance during phases that are interpreted as climatic transition zones with a shallow water cover as for example in two horizons that frame the extremely dry YD. Supporting this interpretation *Melanoides tuberculata* has been established as a strong indicator for the presence of a shallow lake, as it prefers a littoral habitat with aquatic and subaquatic plants (Pointier et al., 1992; Leng et al., 1999) in up to 2 m water depth with a tolerance to max. 10–15 m water cover. Fish bones are found

episodically in a clayey matrix throughout the cores (Fig. 3), but are also deposited densely in some sharply defined layers that seem to correlate with a receding lake (e.g. end of the pre-YD lake phase and the pre-H1 lake phase recorded in 4.32–4.39 m in CB-05, correlating with fossilised fish remains in CB-03 at 7.38 and 7.68 m). Diatoms (Figs. 4 and 5) in both cores are restricted to the horizon that can roughly be attributed to the AHP lake phase (CB-03: 1.90–5.10 m; CB-05: 1.12–3.10 m; Fig. 3), with slightly changing taxa spectra within that layer. The spectrum comprises both, centric and pennate species, with a clear dominance of the genera *Aulacoseira* and *Cyclostephanus*. Furthermore, species of the genera *Nitzschia*, *Synedra*, *Cymbella*, *Cyclotella* and *Achnanthes* could be identified, with the more habitat specific species restricted to the stable fresh water lake phase. *Aulacoseira* with a broader alkalinity and salinity tolerance occur almost throughout the entire section with diatoms and show dominance during shallow lake phases. The YD interval that caused the paleo-lake CB to regress to shallow and presumably highly saline and alkaline pools, is marked by a sharp decline of preserved frustules, expressed in the disappearance of diatom occurrences at the margin of the basin and the reduction to very few *Aulacoseira* frustules/no diatoms at all in that section. After the YD, with the reestablishment of a freshwater lake, diatoms are quickly found again in great abundance and an increased variety of species for the entire AHP phase. This is also expressed in the Si curve reflecting the increase of biogenic silica in the lake by the autogenic production of silica rich frustules (Fig. 3).

5 Interpretation of proxies during a complete dry-wet cycle

Figure 4 shows a conceptual model of the physical and chemical responses of the Chew Bahir basin to wet and dry conditions.

During arid phases in Chew Bahir (Fig. 4), we postulate a desiccated or strongly regressed lake, framed by a higher lithogenic fraction, and a lower productivity, high K due to the dominance of physical weathering and activation of alluvial fans transporting

K from the constrained source in the western part of the catchment (i.e., the Hammar Range, Fig. 1) and lesser dilution. *During wet phases*, we postulate a freshwater lake with max. 50 m water level, fine grain deposits, freshwater diatom occurrences, high Cl (most likely due to enhanced chemical weathering), and low K due to a dense vegetation cover on the slopes of the Hammar range (and the whole catchment area) strongly restricting the erosion of K-bearing weathered products into the basin. Sharp Ca peaks mark the onset of wet conditions, while their terminations (and onsets) are mostly accompanied by rich mollusc occurrences that require shallow-water habitats (max. 10–15 m). The main input system is fluvial, with the major provenance of deposits being northern, northeastern and northwestern catchment, depending on the magnitude of humidity.

Comparing the climate records CB01, CB03 and CB05 from Chew Bahir (Fig. 6), derived from different proxies and from different sites in the same archive, it becomes apparent that the deposits have largely recorded the same climatic events, though with differing expressions. We postulate that minor lead or lags in the responses and the abruptness of the shifts are enhanced by proxy specificity, whereas the magnitude of the climate signal recorded in the CB deposits are site specific.

The onset of the AHP for example, illustrates the mechanism that is controlling the shifts in the Cl and the K record. Especially in CB-03, the proxy specific response towards moisture increase becomes apparent: whereas humidity proxy Cl indicates an *increase of moisture* by increased values, the K record shows a multiple enhanced response, as the dilution effect drives a rapid *drop* of elemental counts. Thus the aridity proxy K shows an intensified response to the increase of moisture availability by *decreased* values. However, both proxies show that a clear shift from dry to wet has been recorded aside from the nature of the chosen proxy. The same is applicable for the return to humid conditions at the end of the YD: in CB-03 for instance, the response of K to increased moisture influx is more pronounced then in Cl, although again both proxies indicate an alternation dry to wet. The reversed principle can be applied to the shift from wet to dry as shown for the onset of arid conditions during the YD: here

humidity proxy Cl reacts more sensitively and shows an enhanced response. Whereas the increase of K in the deposits seems less sharply defined as here an actual increase in K-bearing weathering products is the major mechanism driving the shift instead of dilution by a developing water body. The aim of these findings is to illustrate that it is important to understand that for a climatic reconstruction both proxies are evaluated as reliable and sensitive climate indicators, but each has important peculiarities that need to be considered when discussing climatic history.

The proxies are controlled by three major factors bound in a complex interplay: distance to and restriction of the source (provenance), prevailing erosion and transport mechanism (fluvial, alluvial fan activity, aeolian) that is heavily influenced by density and type of vegetation and weathering (chemical vs. mechanical).

Comparing the same dry-wet alternations named above in between the cores in Fig. 6, makes clear that each coring site although just a few km apart and all belonging to the same sedimentary archive in the same catchment, still show remarkable site specific expressions. We assume the shifting dominance of the transport and erosional mechanisms to be responsible for that. Whereas CB-01 at the marginal area of the basin has a 2–3 fold resolution, is controlled by less processes and has a restricted provenance, CB-05 in the middle of the paleo-lake Chew Bahir has been subdued to redistribution processes in the former lake as both, the sedimentary composition and the partially overprinted elemental record during lake-phases indicate. But again, all cores show the major dry-wet cycles and mostly the short-term climate events that are discussed in the following chapter. By integrating the results from all three areas in the basin in the following discussion, we essay to provide cross control to avoid misinterpretation of one bore site-specific disturbance in the deposits as an actual climate event.

6 Discussion of climatic variability recorded in Chew Bahir

The Chew Bahir records provide insights into the velocity and character of wet-dry-wet transitions over the past 46 000 yr in the source region of AMH on different time scales. Three different modes were identified showing variability on precessional, millennial as well as decadal time scales all characterized by either abrupt or gradual changes of different magnitudes, which will be discussed in detail within the next chapter using the potassium record as a representative proxy of the studied records.

6.1 Variability on orbital time scales

On long-term times scales (10^4 yr), the Chew Bahir records cover the last two precessional cycles, which are generally understood as the main controlling factor for long-term moisture variability in Africa (e.g., Gasse, 2000; Gasse and Van Campo, 2001; Trauth et al., 2001, 2003; Barker et al., 2004) (Fig. 7). Hence, the AHP (~15–5 ka BP) represents a textbook example for orbital driven moisture increase during a precessional minimum. This orbital configuration that is associated with higher insolation values in June–August (JJA) for the Northern Hemisphere (e.g., Laskar et al., 2004) has caused (a) the displacement of the ITCZ during JJA further north, bringing more moisture to regions that are usually not under the influence of the ITCZ, such as in the Sahara or Oman (e.g., Burns et al., 1998; Hoelzmann et al., 2000; Neff et al., 2001; Lancaster et al., 2002), (b) a stronger West African Summer Monsoon (WAM) associated with a weakening of the African easterly jet that is responsible for the export of moisture out of Africa (e.g., Patricola and Cook, 2007) and (c) a shift of the CAB eastwards, over the highly-elevated plateaus of East Africa, therewith contributing to the synchronous character observed in the rise of lake levels in the basins of the EARS up to their overflow levels (Tierney et al., 2011; Costa et al., 2014; Junginger et al., 2014). Though, as recently shown by Junginger and Trauth (2013), the influence of the CAB during the last dry-wet cycle, has been restricted to phases with the highest Indian Summer monsoon activity (~14.8–7.8 ka BP) due to constraints imposed by an atmospheric pressure gradient between Asia and East Africa.

The timing and foremost the character of both transitions, in and out of the AHP, are highly debated (e.g. deMenocal et al., 2000; Kröpelin et al., 2008). In the Chew Bahir basin, the onset of the AHP occurred abruptly (less than 500 yr) as indicated by the K record (Fig. 7), and also by the proxies Cl, Ti, Fe, Ca and fossil occurrences (Figs. 3 and 6). These findings from Chew Bahir are synchronous with other sites in East Africa, despite the gradual increase in boreal summer (JJA) insolation (Gasse, 2000; Junginger et al., 2014) that would suggest a likewise gradual transition in moisture availability. Nor did the termination of the AHP in Chew Bahir follow the linear decline of NH summer (JJA) insolation. Instead, taking all three coring sites (CB01, CB03, CB05) in Chew Bahir into account, the record suggests the onset of the Holocene aridification trend at ~6.5 ka BP, gradually reaching full arid conditions earliest at ~5 ka BP (Figs. 6 and 7). This indicates a slightly lagged and disproportionally gradual decline of moisture availability in Chew Bahir as compared to the decrease in insolation.

The non-linear character and temporal offset of the AHP transitions in the EARS have been related to a complex interplay of several factors: changes in precession, changes in the general source of moisture and boundary conditions imposed by the extent of NH ice sheets.

In detail, it has been hypothesized that moisture availability towards the end of the AHP in tropical Africa was prolonged despite the decline in the NH summer insolation maximum due to a change in precession leading to a higher insolation in October–November (ON) at the equator (Marzin and Braconnot, 2009; Junginger et al., 2014). This latitudinal change in higher insolation values from maximum values during summer months for the NH to increased insolation values for ON at the equator (Fig. 7) was tied to a fundamental change in moisture sources. The CAB was prevented then from reaching the EARS – including Chew Bahir – by the reorganisation of atmospheric pressure, but instead more moisture became available during the short rainy season in ON carried via the ITCZ (Junginger and Trauth, 2014). As explained in these studies, despite the comparatively enhanced moisture availability during the short rainy season, the provided moisture was not sufficient anymore to sustain the high lake levels in

the EARS as observed during NH summer insolation maxima. This change caused a delayed but gradual decline of the lakes at the termination of the AHP following ON insolation (Fig. 7). Moreover, the role of the dense vegetation cover that could develop during the long humid phase would have saved moisture within the system and thus might have also contributed to the delay of the precession driven aridification process.

For the equatorial insolation maximum during the long rainy season from March to May (MAM), that has occurred at ~22–16 ka BP we would theoretically expect a similar scenario as described above. The Chew Bahir climate records of CB01 and CB03 show a clear though moderate tendency towards more humid conditions slightly differing in their character but distinctly following the March–May equatorial insolation maximum (Fig. 7). But in contrast to the termination of the AHP, the equatorial MAM insolation – although preceding maximum JJA NH insolation – is not leading to a gradual transition into the full humid conditions marking the onset of the AHP. This could be attributed to the fact that these equatorial insolation maxima in spring (MAM) coincide with the Last Glacial Maximum (LGM, 23–18 ka) that is known to have caused a reduction in moisture fluxes in the atmosphere on a global scale due to colder temperatures (Gasse, 2000). This generally low moisture availability is also reflected in numerous low-latitude sites showing a phase of pronounced aridity (e.g., Gasse, 2000; Barker et al., 2004), although the orbital parameters would predict increased rainfall. This implies that for the LGM interval, precipitation in Chew Bahir could have been controlled by high-latitude ice sheet coverage more than by the equatorial insolation alternations.

Moreover, the extent of NH ice sheets most likely largely contributed to the delayed, but then abrupt response of East African lake levels to the increase of NH summer insolation (Gasse, 2000). This approach states a threshold, assuming that a particular stage of ice cover retreat is necessary, to allow for the development of distinct atmospheric pressure gradients which in turn are steep enough for the CAB to be shifted eastwards and thus decidedly modulating the rapid establishment of deep lakes (Junginger and Trauth, 2013; Costa et al., 2014) in East Africa.

When extrapolating those three preconditions that significantly modulated the AHP to the penultimate precessional cycle (~46–23 ka) (Fig. 7), we would expect to see a similar expression in the records of Chew Bahir as during the last orbitally controlled wet-dry cycle, in particular for the intervals during insolation maxima at the equator in MAM and ON and NH JJA insolation maxima. However, the penultimate precessional cycle could above all be characterised as a rather long dry episode, reflecting the reduced atmospheric pressure gradients and reduced moisture that heavily buffered the impact of orbital parameters on the East African climate during the last glacial (Gasse, 2000).

6.2 Variability on millennial time scales

Despite the climate's overall arid character during MIS 3 (our core covers 46–23 ka BP), we observe abrupt short-term excursions from this level of aridity towards more humid conditions in southern Ethiopia, lasting between ~500–1000 yr with one exception at 42.5–40.5 ka BP that lasted ~2000 yr. The timing, duration and character of these dry-wet shifts strongly resemble the high-latitude millennial-scale climate oscillations (Fig. 7) during the last glacial that are known as Dansgaard–Oeschger cycles (D-O). Those show distinctively abrupt excursions towards warmer temperatures followed by gradual saw-toothed cooling trends (e.g. Dansgaard et al., 1993; Braun et al., 2005). Furthermore, several millennial scale climatic events, later named Heinrich-events (H0–H6) that were first documented in ice-rafted debris in the North Atlantic, are known to have left a global footprint that is mostly coinciding with dry spells in low-latitude Africa (Fig. 7; Heinrich, 1988; Bond and Lotti, 1995; Hemming, 2004; Jullien et al., 2007) and that could be expressed in several dry phases in the Chew Bahir record. Besides the clear evidence of these millennial scale climate variations we see in the Chew Bahir record, here expressed in oscillations between wet and dry instead of warm and cold, similar expressions can also be observed in the SST reconstructions from the tropical and mid-latitude East Atlantic (Martrat et al., 2007; Mulitza et al., 2008), vegetation changes in the Balkans (Panagiotopolus et al., 2013), short-term variations

in the WAM (Overpeck et al., 1996) and also changes in the ocean productivity due to changes in the ISM strength in the Arabian Sea (Altabet et al., 2002). Although there is no consensus yet concerning possible triggering mechanisms for both, D-O cycles and H-events, or whether there is even a common ultimate driver for all events, some studies suggest that these abrupt shifts have been associated with changes in the solar irradiation on millennial to centennial time-scales causing rapid reorganisations in the atmospheric systems (e.g., Braun et al., 2005). Hemming et al. (2004) conclude that besides jökulhlaups (glacial outburst floods) and ice sheet build-ups/collapses, glaciological instability is the most likely mechanism behind the H-events. Whether the millennial cycles or the pronounced shifts in Chew Bahir lead or lag high-latitude events is not clear, that's why we refrain from pairing designated D-O cycles to the millennial dry-wet cycles that are distinct in the CB record. Therefore we cannot contribute to debate on whether possibly low-latitude forcing could be the triggering factor of these events.

The most recent and rather sharply defined wet interval on a millennial time scale interrupts the mid-late Holocene dry phase between 2.2 and 1.3 ka BP, in character and magnitude resembling the D-O events as observed during the glacial. This excursion to humid conditions could possibly also be related to pronounced short-term changes in the solar activities (Solanki et al., 2004), despite occurring during an interglacial.

There are two similar climate events that occurred during the AHP (thus full humid conditions), but featuring with a distinctive shift towards major drought conditions a seemingly reversed character: a major arid event around 14 ka BP in Chew Bahir resembles a synchronous decline in Lake Victoria (Stager et al., 2002) that was interpreted as the tropical African expressions of the cold European Older Dryas (OD) event otherwise sparsely documented for low-latitudes. The most prominent and sharply defined dry phase in the CB record that occurs between 12.8 and 11.6 ka BP and therewith closely coincides with the H0-event (Bond and Lotti, 2005) or Younger Dryas chronozone that is well documented to have caused extreme arid conditions in a series of sites in Africa north of 10° S (e.g. Barker et al., 2004). Also the internal

variability within the YD (e.g. Liu et al., 2013), with at least two wet excursions, is distinct in our CB record (Fig. 7). The return to full humid conditions occurred abruptly within ±200 yr, as indicated by the humidity sensitive K record, a freshwater diatom flora and the sensitive Ca marker peaks and is also consistent with other records in East Africa north of 10° S (Gasse, 2000; Barker et al., 2004; Junginger et al., 2014).

Aside from the underlying driving mechanisms, the question remains whether the moisture that was provided by these millennial-scale wet periods was sufficient to allow the establishment of open fresh water lakes, crucial for the survival of mammals including the AMH or whether the enhanced moisture did in fact not exceed evaporation, merely leaving small and alkaline lakes behind. Barker et al. (2004) has shown that central Kenyan lakes have remained alkaline although exceeding present day levels during moisture periods within the last glacial.

6.3 Variability on centennial–decadal time scales

The K record also shows clearly decadal to centennial scale short-term events punctuating the AHP by several dry intervals, such as at ~10.5, ~9.5, 8.15–7.8, and ~7 ka BP (Fig. 7). These drought events correlate within a small error range with records implying the weakening of the ISM (Neff et al., 2001; Gupta et al., 2005; Wang et al., 2005), increased iceberg discharges in the NH (Bond et al., 2001), reduced precipitation in West and Central Africa (Stager et al., 2002; Weldeab et al., 2007) as well as considerable regressions of several lakes in the EARS with falling lake levels of up to −120 m (e.g., Gasse, 2000; Stager et al., 2002; Brown and Fuller, 2008; Junginger et al., 2014). These events that have been observed on a global scale have been associated with short-term changes in solar activity (Solanki et al., 2004), although the exact physical process still remains poorly understood (Gray et al., 2010).

The event between ~8.15–7.8 ka BP however, differs from the other high-frequency drought events in the record due to its gradual drying character of over ~350 yr. The gradual drying trend is also observed in other low latitude records (e.g., Fleitmann et al., 2003; Dykoski et al., 2005; Gupta et al., 2005; Weldeab et al., 2007) and is widely

assumed to predate the abrupt cooling event at 8.2 ka BP in the NH (e.g., Alley et al., 1997). Lake level reconstructions in the EARS revealed pronounced lake regressions up to almost full desiccations (Gillespie et al., 1983; Gasse, 2000; Garcin et al., 2012; Junginger et al., 2014).

The gradual (1500-yr long) aridification trend at the end of the AHP starting at ~6.5 ka ago in southern Ethiopia is also punctuated by several minor 20–80 yr long dry events as observed by Trauth et al. (in review JHE) indicating that even gradual transitions can be influenced by short-term droughts affecting several generations of the AMH. The possible explanation for these fluctuations remains unclear.

7 Conclusions and outlook

The Chew Bahir transect covers the environmental history of the last 46 000 yr, reflecting dry-wet cycles on timescales from ten to ten thousand years. The transitions of these dry-wet alternations are diverse and on all timescales we observe climatic shifts that occur within just a few years as well as extremely gradual transitions. Each coring site within the basin shows individual characteristics, governed by alternating fluvial and lacustrine dynamics, but show clear conformity in geochemical, physical and biological proxies. The interpretation of our multi-proxy data and the final comparison between the coring sites provides us with a basic concept of how Chew Bahir has responded to moisture variability. This conceptual understanding represents a fundamental basis for the interpretation of the to-be cored 400 m long sequence from Chew Bahir within the framework of the HSPDP (Cohen et al., 2009). Based on this study, this 400 m record is conservatively estimated to cover at least the last 500 ka and therewith the crucial climatic and environmental changes through the critical intervals of human evolution.

The timing, magnitude and character of the wet-dry-wet transitions would have had important consequences for humans. A longer transition phase would allow a longer period to adapt to a changing environment, given that the impact and frequency of internal variations do not cross a threshold that marks inhabitable environmental

conditions. On the other hand, the abrupt onset of wet conditions as reconstructed for the transition into the AHP for example could have been accompanied by flooding. The extremely variable environment as reconstructed for the D-O cycles during the last glacial would have meant a dramatic environmental change from possibly full humid conditions enabling lush flora and lakes back to an extremely dry climate with a desiccated lake and clearly limited food resources. So the climatic impact factor in the human-environmental interaction seems to be determined mainly by the magnitude and duration of a cycle as well as the timespan to swing from one condition to the other extreme. However, this idea does not take the human decision-making, social and cultural concepts into account. To test what impact climatic change on decadal to millennial time scales might have had on settlement activities and cultural shifts towards environment adapted innovations, a parallel work compares the climate history of the last 20 ka BP from Chew Bahir with the archaeological record of adjacent hypothesised refugia (Foerster et al., 2014).

However, to get beyond this still mostly hypothetical interpretation of our data and possible mechanisms involved at this point of research, it is necessary to firstly, further improve and validate our understanding about the provenance, weathering and transport mechanisms from source to the actual deposits in the cores. Secondly, studies using isotopes could clarify beyond the well-established K record the actual extend and provenance of freshwater in paleo-lake Chew Bahir and help to reconstruct the now hypothesised different moisture sources reaching the study area.

Acknowledgements. We thank Addis Ababa University for making the realisation of the field campaign in difficult terrain possible. We are grateful for the great commitment of Oliver Langkamp and Wolfgang Frank, without whose we would not have such core material. We thank Jonas Urban, Jan Wowrek, Diana Becker, Stefanie Rohland for dedicated assistance in the lab. We thank Karsten Schittek, Tsige Kassa, Jonathan Hense, Kostas Panagiotopoulos, J. P. Francois for their advise and fruitful discussions, Nicole Mantke (University of Cologne), Oliver Oswald (University of Potsdam) for (long distance) help and advise with the Potsdam XRD analysis and Johannes Jakob (University of Cologne) for very patient support related to the technical introduction into MSCL Logging. We thank Volker Wennrich for support with the

XRF scanning procedure and advise related to the geochemical interpretation. This project is affiliated to the CRC 806 (A3 project), which financially supported the first field campaign in 2009 that produced the pilot core, fundamental for this work. The Chew Bahir Project is a contribution to the International Continental Scientific Drilling Program (ICDP), part of the ICDP-HSPDP initiative lead by A. Cohen. Analyses regarding planetary magnetisms were funded by DFG SPP 1488. ICDP supported the second field campaign in 2010 when we cored CB site 02 to 06. We thank the German Science Foundation (DFG) for funding all these projects. This paper is dedicated to our colleague Mohammed Umer.

References

Allen, J. R. M., Watts, W. A., and Huntley, B.: Weichselian palynostratigraphy, palaeovegetation and palaeoenvironment; the record from Lago Grande di Monticchio, southern Italy, Quatern. Int., 73–74, 91–110, 2000.

Alley, R. B., Mayewski, A., Sowers, T., Stuiver, M., Taylor, K. C., and Clark, P. U.: Holocene climatic instability: a prominent, widespread event 8200 years ago, Geology, 25, 483–486, 1997.

Altabet, M. A., Higginson, M. J., and Murray, D. W.: The effect of millennial-scale changes in Arabian Sea denitrification on atmospheric CO_2, Nature, 415, 159–162, 2002.

Ambrose, S. H.: Late Pleistocene human population bottlenecks, volcanic winter, and the differentiation of modern humans, J. Hum. Evol., 35, 115–118, 1998.

Awoke, H. and Hailu, F.: Geology of the Yabello Area, Geological Survey of Ethiopia, Addis Ababa, 2004.

Barker, P. A., Talbot, M. R., Street-Perrott, F. A., Marret, F., Scourse, J., and Odada, E. O.: Late quaternary variability in intertropical Africa, in: Past Climate Variability through Europe and Africa, edited by: Battarbee, R. W., Gasse, F., and Stickley, C. E., Springer, Dordrecht, the Netherlands, 117–138, 2009.

Berger, A. and Loutre, M.-F.: Insolation values for the climate of the last 10 million years, Quaternary Sci. Rev., 10, 297–317, 1991.

Björck, S. and Wohlfarth, B.: ^{14}C chronostratigraphic techniques in paleolimnology, in: Tracking Environmental Change Using Lake Sediments Volume 1: Basin Analysis, Coring, and

Chronological Techniques, edited by: Last, W. and Smol, J., Springer, Dordrecht, the Netherlands, 205–246, 2001.

Blaauw, M. and Christen, J. A.: Flexible paleoclimate age-depth models using an autoregressive gamma process, Bayesian Analysis, 6, 457–474, doi:10.1214/11-BA618, 2011.

Bond, L. and Lotti, R.: Iceberg discharges into the North Atlantic on millennial time scales during the last glaciation, Science, 267, 1005–1010, 1995.

Braun, H., Christl, M., Rahmstorf, S., Ganopolski, A., Mangini, A., Kubatzki, C., Roth, K., and Kromer, B.: Possible solar origin of the 1470-year glacial climate cycle demonstrated in a coupled model, Nature, 438, 208–211, 2005.

Bronk Ramsey, C.: Deposition models for chronological records, Quaternary Sci. Rev., 27, 42–60, 2008.

Bronk Ramsey, C.: Bayesian analysis of radiocarbon dates, Radiocarbon, 51, 337–360, 2009.

Bronk Ramsey, C.: OxCal v4.1.7 Calibration Software, available at: http://c14.arch.ox.ac.uk/ (last access: 19 November 2013), 2010.

Brown, E. T. and Fuller, C. H.: Stratigraphy and tephra of the Kibish Formation, southwestern Ethiopia, J. Hum. Evol., 55, 366–403, 2008.

Brown, M. C., Frank, U., Foerster, V.; Kassa, T., Nowaczyk, N., Schäbitz, F., and Korte, M.: Holocene paleomagnetic field variations recorded in lake sediments from southern Ethiopia, AGU Fall Meeting, San Francisco, USA, 3–7 December 2012, GP33B-01, 2012.

Burnett, A. P., Soreghan, M. J., Scholz, C. A., and Brown, E. T.: Tropical East African climate change and its relation to global climate: a record from Lake Tanganyika, tropical East Africa, over the past 90+kyr, Palaeogeogr. Palaeocl., 303, 155–167, 2011.

Burns, S. J., Matter, A., Frank, N., and Mangini, A.: Speleothem-based paleoclimate record from northern Oman, Geology, 26, 499–502, 1998.

Camberlin, P.: Rainfall anomalies in the source region of the Nile and their connection with the Indian summer monsoon, J. Climate, 10, 1380–1392, 1997.

Carto, S. L., Weaver, A. J., Hetherington, R., Lam, Y., and Wiebe, E. C.: Out of Africa and into an ice age: on the role of global climate change in the late Pleistocene expansion of early modern humans out of Africa, J. Hum. Evol., 56, 139–151, 2009.

Castañeda, I. S., Mulitza, S., Schefuß, E., Santos, R. A. L., Damste, J. S. S., and Schouten, S.: Wet phases in the Sahara/Sahel region and human expansion patterns in North Africa, P. Natl. Acad. Sci. USA, 106, 1–5, 2009.

Cohen, A., Arrowsmith, R., Behrensmeyer, A. K., Campisano, C., Feibel, C., Fisseha, S., Johnson, R., Kubsa Bedaso, Z., Lockwood, C., Mbua, E., Olago, D., Potts, R., Reed, K., Renaut, R., Tiercelin, J.-J., and Umer, M.: Understanding paleoclimate and human evolution through the hominin sites and paleolakes drilling project, Scientific Drilling, 8, 60–65, doi:10.2204/iodp.sd.8.10.2009, 2009.

Cohen, A. S.: Paleolimnology: The History and Evolution of Lake Ecosystems, Oxford University Press, Oxford, 500 pp., 2003.

Corti, G.: Continental rift evolution: from rift initiation to incipient break-up in the Main Ethiopian Rift, East Africa, Earth-Sci. Rev., 96, 1–53, 2009.

Costa, K., Russell, J., Konecky, B., and Lamb, H.: Isotopic reconstruction of the African humid period and Congo air boundary migration at Lake Tana, Ethiopia, Quaternary Sci. Rev., 83, 58–67, 2014.

Croudace, I. W., Rindby, A., and Rothwell, R. G.: ITRAX: description and evaluation of a new X-ray core scanner, in: New Ways of Looking at Sediment Cores and Core Data, edited by: Rothwell, R. G., Geological Society Special Publication, 267, London, UK, 51–63, 2006.

Dansgaard, W., Johnson, S. J., Clausen, H. B., Dahl-Jensen, D., Gundestrup, N. S., Hammer, C. U., Hvidberg, C. S., Steffensen, J. P., Sveinbjornsdottir, A. E., Jouzel, J., and Bond, G.: Evidence for general instability of past climate from a 250-kyr ice-core record, Nature, 364, 218–220, 1993.

Davidson, A.: The Omo River project: reconnaissance geology and geochemistry of parts of Ilubabor, Kefa, Gemu Gofa and Sidamo, Ethiopian Institute of Geological Surveys Bulletin, 2, 1–89, 1983.

deMenocal, P., Ortiz, J., Guilderson, T., Adkins, J., Sarnthein, M., Baker, L., and Yarusinsky, M.:. Abrupt onset and termination of the African humid period: rapid climate responses to gradual insolation forcing, Quaternary Sci. Rev., 19, 347–361, 2000.

Dykoski, C. A., Edwards, R. L., Cheng, H., Yuan, D., Cai, Y., Zhang, M., Lin, Y., Qing, J., An, Z., and Revenaugh, J.: A high-resolution, absolute dated Holocene and deglacial Asian monsoon record from Dongge Cave, China, Earth Planet. Sc. Lett., 233, 71–86, 2005.

Ebinger, C. J., Yemane, T., Harding, D., Tesfaye, S., Kelley, S., and Rex, D.: Rift deflection, migration, and propagation: linkage of the Ethiopian and Eastern rifts, Africa, Geol. Soc. Am. Bull., 112, 163–176, 2000.

Felton, A. F., Russell, J. M., Cohen, A. S., Baker, M. E., Chesley, J. T., Lezzar, K. E., McGlue, M. M., Pigati, J. S., Quade, J., Stager, J. C., and Tiercelin, J. J.: Paleolimnological

evidence for the onset and termination of glacial aridity from Lake Tanganyika, Tropical East Africa, Palaeogeogr. Palaeocl., 252, 405–423, 2007.

Fleitmann, D., Burns, S. J., Mudelsee, M., Neff, U., Kramers, J., Mangini, A., and Matter, A.: Holocene forcing of the Indian monsoon recorded in a stalagmite from Southern Oman, Science, 300, 1737–1739, 2003.

Foerster, V., Junginger, A., Langkamp, O., Gebru, T., Asrat, A., Umer, M., Lamb, H., Wennrich, V., Rethemeyer, J., Nowaczyk, N., Trauth, M. H., and Schäbitz, F.: Climatic change recorded in the sediments of the Chew Bahir basin, southern Ethiopia, during the last 45,000 years, Quatern. Int., 274, 25–37, doi:10.1016/j.quaint.2012.06.028, 2012.

Frank, U., Brown, M., Foerster, V., and Schäbitz, F.: Paleomagnetism of Lake Sediments, Chew Bahir, Ethiopia, AGU Fall Meeting, San Francisco, USA, 5–9 December 2011, GP43A-04, 2011.

Garcin, Y., Melnick, D., Strecker, M. R., Olago, D., and Tiercelin, J.-J.: East African mid-Holocene wet–dry transition recorded in palaeo-shorelines of Lake Turkana, northern Kenya Rift, Earth Planet. Sc. Lett., 331–332, 322–334, 2012.

Gasse, F.: Hydrological changes in the African tropics since the last glacial maximum, Quaternary Sci. Rev., 19, 189–211, 2000.

Gasse, F. and Van Campo, E.: Abrupt post-glacial climate events in West Asia and North Africa monsoon domains, Earth Planet. Sc. Lett., 126, 435–456, 1994.

Geyh, M. A., Schotterer, U., and Grosjean, M.: Temporal changes of the (super 14) C reservoir effect in lakes, Radiocarbon, 40, 921–931, 1998.

Govin, A., Holzwarth, U., Heslop, D., Ford Keeling, L., Zabel, M., Mulitza, S., Collins, J. A., and Chiessi, C. M.: Distribution of major elements in Atlantic surface sediments (36° N–49° S): Imprint of terrigenous input and continental weathering, Geochem. Geophy. Geosy., 13, 1–23, 2012.

Gray, L. J., Beer, J., Geller, M., Haigh, J. D., Lockwood, M., Matthes, K., Cubasch, U., Fleitmann, D., Harrison, G., Hood, L., Luterbacher, J., Meehl, G. A., Shindell, D., van Geel, B., and White, W.:, Solar influences on climate, Rev. Geophys., 48, RG4001, doi:10.1029/2009RG000282, 2010.

Gupta, A. K., Das, M., and Anderson, D. M.: Solar influence on the Indian summer monsoon during the Holocene, Geophys. Res. Lett., 32, L17703, doi:10.1029/2005GL022685, 2005.

Heinrich, H.: Origin and consequences of cyclic ice rafting in the Northeast Atlantic Ocean during the past 130,000 years, Quaternary Res., 29, 142–152, 1988.

Hemming, S. R.: Heinrich events: massive late Pleistocene detritus layers of the North Atlantic and their global climate imprint, Rev. Geophys., 42, 1–43, 2004.
Hildebrand, E. and Grillo, K.: Early herders and monumental sites in eastern Africa: new radiocarbon dates, Antiquity, 86, 338–352, 2012.
Hildebrand, E., Brandt, S., and Lesur-Gebremariam, J.: The Holocene archaeology of Southwest Ethiopia: new insights from the Kafa archaeological project, Afr. Archaeol. Rev., 27, 255–289, 2010.
Hoelzmann, P., Kruse, H., and Rottinger, F.: Precipitation estimates for the eastern Saharan palaeomonsoon based on a water balance model of the West Nubian Palaeolake Basin, Global Planet. Change, 26, 105–120, 2000.
IRI (International Research Institute for Climate and Society), Earth Institute, Columbia University, Climate and Society Maproom available at: http://iridl.ldeo.columbia.edu/maproom/ (last access: 4 October), 2013.
Jullien, E., Grousset, F., Malaizé, B., Duprat, J., Sanchez-Goni, M. F., Eynaud, F., Charlier, K., Schneider, R., Bory, A., Bout, V., and Flores, J. A.: Low-latitude "dusty events" vs. high-latitude "icy Heinrich events", Quaternary Res., 68, 379–386, 2007.
Junginger, A. and Trauth, M. H.: Hydrological constraints of paleo-Lake Suguta in the northern Kenya Rift during the African humid period (15–5 ka BP), Global Planet. Change, 111, 174–188, 2013.
Junginger, A., Roller, S., Olaka, L. A., and Trauth, M. H.: The effect of solar radiation changes on water levels in paleo-Lake Suguta, Northern Kenya Rift, during late Pleistocene African Humid Period (15–5 ka BP), Paleogeography, Paleoclimatology, Paleoecology, 396, 1–16, 2014.
Johnson, T. C., Halfman, J. D., and Showers, W. J.: Paleoclimate of the past 4000 years at Lake Turkana, Kenya, based on the isotopic composition of authigenic calcite, Palaeogeogr. Palaeocl., 85, 189–198, 1991.
Key, R. M.: Geology of the Sabarei area: Degree sheets 3 and 4, with coloured 1:250 000 geological map and results of geochemical exploration (Report), Ministry of Environment and Natural Resources, Mines and Geology Dept., Nairobi, Kenya, 1988.
Kliem, P., Enters, D., Hahn, A., Ohlendorf, C., Lisé-Pronovost, A., St-Onge, G., Wastegård, S., Zolitschka, B., and the PASADO Science Team: Lithology, radiocarbon chronology and sedimentological interpretation of the lacustrine record from Laguna Potrok Aike, southern Patagonia, Quaternary Sci. Rev., 71, 54–62, 2013.

Kröpelin, S., Verschuren, D., Lézine, A.-M., Eggermont, H., Cocquyt, C., Francus, P., Cazet, J.-P., Fagot, M., Rumes, B., Russell, J. M., Darius, F., Conley, D. J., Schuster, M., von Suchodoletz, H., and Engstrom, D. R.: Climate-driven ecosystem succession in the Sahara: the past 6000 years, Science, 320, 765–768, 2008.
Lancaster, N., Kocurek, G., Singhvi, A., Pandey, V., Deynoux, M., Ghienne, J.-F., and Lô, K.: Late Pleistocene and Holocene dune activity and wind regimes in the western Sahara Desert of Mauritania, Geology, 30, 991–994, 2002.
Laskar, J., Gastineau, M., Joutel, F., Robutel, P., Levrard, B., and Correia, A.: A long term numerical solution for the insolation quantities of Earth, Astron. Astrophys., 428, 261–285, 2004.
Leng, M. J., Lamb, A. L., Lamb, H. F., and Telford, R. J.: Palaeoclimatic implications of isotopic data from modern and early Holocene shells of the freshwater snail *Melanoides tuberculata*, from lakes in the Ethiopian Rift Valley, J. Paleolimnol., 21, 97–106, 1999.
Levin, N. E., Zipser, E. J., and Cerling, T. E.: Isotopic composition of waters from Ethiopia and Kenya: insights into moisture sources for eastern Africa, J. Geophys. Res., 114, D23306, doi:10.1029/2009JD012166, 2009.
Martrat, B., Grimalt, J. O., Shackleton, N. J., de Abreu, L., Hutterli, M. A., and Stocker, T. F.: Four climate cycles of recurring deep and surface water stabilizations on the Iberian margin, Science, 317, 502–507, doi:10.1126/science.1142964, 2007.
Marzin, C. and Braconnot, P.: Variations of Indian and African monsoons induced by insolation changes at 6 and 9.5 kyr BP, Clim. Dynam., 33, 215–231, 2009.
Maslin, M. A. and Trauth, M. H.: Plio-Pleistocene East African pulsed climate variability and its influence on early human evolution, in: The First Humans – Origins of the Genus Homo, Vertebrate Paleobiology and Paleoanthropology Series, edited by: Grine, F. E., Leakey, R. E., and Fleagle, J. G., Springer Verlag, Dordrecht, the Netherlands, 151–158, 2009.
McDougall, I., Brown, F. H., and Fleagle, J. G.: Stratigraphic placement and age of modern humans from Kibish, Ethiopia, Nature, 433, 733–736, 2005.
Meyers, P. A.: Applications of organic geochemistry to paleolimnological reconstructions: a summary of examples from the Laurentian Great Lakes, Org. Geochem., 34, 261–289, 2003.
Mulitza, S., Prange, M., Stuut, J.-B., Zabel, M., von Dobeneck, T., Itambi, A. C., Nizou, J., Schulz, M., and Wefer, G.: Sahel megadroughts triggered by glacial slowdowns of Atlantic meridional overturning, Paleoceanography, 23, PA4206, doi:10.1029/2008PA001637, 2008.

Neff, U., Burns, S. J., Mangini, A., Mudelsee, M., Fleitmann, D., and Matter, A.: Strong coherence between solar variability and the monsoon in Oman between 9 and 6 kyr ago, Nature, 411, 290–293, 2001.

Nicholson, S. E.: A review of climate dynamics and climate variability in eastern Africa, in: The Limnology, Climatology and Paleoclimatology of the East African Lakes, edited by: Johnson, T. C. and Odada, E. O., Gordon & Breach, Amsterdam, the Netherlands, 25–56, 1996.

North Greenland Ice Core Project members: High-resolution record of Northern Hemisphere climate extending into the last interglacial period, Nature, 431, 147–151, 2004.

Ohlendorf, C., Gebhardt, C., Hahn, A., Kliem, P., Zolitschka, B., and the PASADO Science Team: The PASADO core processing strategy – a proposed new protocol for sediment core treatment in multidisciplinary lake drilling projects, Sediment. Geol., 239, 104–115, 2011.

Oppenheimer, S.: The great arc of dispersal of modern humans: Africa to Australia, Quatern. Int., 202, 2–13, 2009.

Overpeck, J., Anderson, D., Trumbore, S., and Prell, W.: The southwest Indian monsoon over the last 18000 years, Clim. Dynam., 12, 213–225, 1996.

Panagiotopoulos, K., Böhm, A., Leng, M. J., Wagner, B., and Schäbitz, F.: Climate variability since MIS 5 in SW Balkans inferred from multiproxy analysis of Lake Prespa sediments, Clim. Past Discuss., 9, 1321–1362, doi:10.5194/cpd-9-1321-2013, 2013.

Patricola, C. M. and Cook, K. H.: Dynamics of the West African monsoon under mid-Holocene precessional forcing: regional climate model simulations, J. Climate, 20, 694–716, 2007.

Pik, R., Marty, B., Carignan, J., Yirgu, G., and Ayalew, T.: Timing of East African Rift development in southern Ethiopia: implication for mantle plume activity and evolution of topography, Geology, 36, 167–170, 2008.

Pointier, J. P., Delay, B., Toffart, J. L., Lefevre, M., and Romero-Alvarez, R.: Life history traits of three morphs of *Melanoides tuberculata* (Gastropoda: Thiaridae), an invading snail in the French West Indies, J. Mollus. Stud., 58, 415–423, 1992.

Potts, R.: Environmental hypotheses of hominin evolution, Yearb. Phys. Anthropol., 41, 93–136, 1998.

Reimer, P. J., Baillie, M. G. L., Bard, E., Bayliss, A., Beck, J. W., Blackwell, P. G., Bronk Ramsey, C., Buck, C. E., Burr, G. S., Edwards, R. L., Friedrich, M., Grootes, P. M., Guilderson, T. P., Hajdas, I., Heaton, T. J., Hogg, A. G., Hughen, K. A., Kaiser, K. F., Kromer, B., McCormac, F. G., Manning, S. W., Reimer, R. W., Richards, D. A., Southon, J. R.,

Talamo, S., Turney, C. S. M., van der Plicht, J., and Weyhenmeyer, C. E.: INTCAL09 and MARINE09 radiocarbon age calibration curves, 0–50,000 years cal BP, Radiocarbon, 51, 1111–1150, 2009.

Segele, Z. T. and Lamb, P. J.: Characterization and variability of Kiremt rainy season over Ethiopia, Meteorol. Atmos. Phys., 89, 153–180, 2005.

Seleshi, Y. and Zanke, U.: Recent changes in rainfall and rainy days in Ethiopia, Int. J. Climatol., 24, 973–983, 2004.

Solanki, S. K., Usoskin, I. G., Kromer, B., Schüssler, M., and Beer, J.: Unusual activity of the sun during recent decades compared to the previous 11,000 years, Nature, 431, 1084–1087, 2004.

Stager, J. C., Mayewski, P. A., and Meeker, L. D.: Cooling cycles, Heinrich event 1, and the desiccation of Lake Victoria, Palaeogeogr. Palaeocl., 183, 169–178, 2002.

Stringer, C.: Out of Ethiopia, Science, 423, 692–694, 2003.

Stuiver, M., Reimer, P. J., and Reimer, R. W.: CALIB 6.0.2html, available at: http://calib.org, last access: 10 July 2013, 2005.

Tierney, J. E. and deMenocal, P. B.: Abrupt shifts in Horn of Africa, hydroclimate since the last glacial maximum, Science, 342, 843–846, doi:10.1126/science.1240411, 2013.

Tierney, J. E., Russell, J. M., Sinninghe Damsté, J. S., Huang, Y., and Verschuren, D.: Late quaternary behavior of the East African monsoon and the importance of the Congo air boundary, Quaternary Sci. Rev., 30, 798–807, 2011.

Tishkoff, S. and Verelli, B.: Patterns of human genetic diversity: implications for human evolutionary history and disease, Annu. Rev. Genom. Hum. G., 4, 293–340, 2003.

Trauth, M. H.: A new probabilitistic technique to determine the best age model for complex stratigraphic sequences, Quat. Geochronol., in review, 2014.

Trauth, M. H., Deino, A., and Strecker, M. R.: Response of the East African climate to orbital forcing during the last interglacial (130–117 ka) and the early last glacial (117–60 ka), Geology, 29, 499–502, 2001.

Trauth, M. H., Deino, A. L., Bergner, A. G. N., and Strecker, M. R.: East African climate change and orbital forcing during the last 175 kyr BP, Earth Planet. Sc. Lett., 206, 297–313, 2003.

Trauth, M. H., Maslin, M. A., Deino, A. L., Junginger, A., Lesoloyia, M., Odada, E. O., Olago, D. O., Olaka, L. A., Strecker, M. R., and Tiedemann, R.: Human evolution in a variable environment: the amplifier lakes of eastern Africa, Quaternary Sci. Rev., 29, 2981–2988, 2010.

Trauth, M. H., Bergner, A., Foerster, V., Junginger, A., Maslin, M., and Schaebitz, F.: Episodes of environmental stability vs. instability in late Cenozoic lake records of eastern Africa, J. Hum. Evol., in review, 2014.

Verschuren, D., Laird, K. R., and Cumming, B. F.: Rainfall and drought in equatorial east Africa during the past 1,100 years, Nature, 403, 410–414, 2000.

Vogelsang, R. and Keding, B.: Climate, culture, and change: from hunters to herders in northeastern and southwestern Africa, in: Comparative Archaeology and Paleoclimatology – Socio-Cultural Responses to a Changing World, BAR International Series, 2456, edited by: Baldia, M. O., Perttula, T. K., and Frink, D. S., Archaeopress, Oxford, UK, 43–62, 2013.

Vrba, E. S.: Environment and evolution: alternative causes of the temporal distribution of evolutionary events, S. Afr. J. Sci., 81, 229–236, 1985.

Wang, Y., Cheng, H., Edwards, R. L., He, Y., Kong, X., An, Z., Wu, J., Kelly, M. J., Dykoski, C. A., and Li, X.: The Holocene Asian monsoon: links to solar changes and North Atlantic climate, Science, 308, 854–857, 2005.

Weber, M., Niessen, F., Kuhn, G., and Wiedcke, M.: Calibration and application of marine sedimentary physical properties using multi-sensor core logger, Mar. Geol., 136, 151–172, 1997.

Weldeab, S., Lea, D. W., Schneider, R. R., and Andersen, N.: Centennial scale climate instabilities in a wet early Holocene West African monsoon, Geophys. Res. Lett., 34, L24702, doi:10.1029/2007GL031898, 2007.

White, T. D., Asfaw, B., DeGusta, D., Gilbert, H., Richards, G. D., Gen Suwa, G., and Howell, C. F.: Pleistocene Homo sapiens from Middle Awash, Ethiopia, Nature, 423, 742–747, 2003.

WoldeGabriel, G. and Aronson, J. L.: Chow Bahir rift: a “failed” rift in southern Ethiopia, Geology, 15, 430–433, 1987.

Table 1. Core locations and core details.

Position within basin	Core ID	Latitude N	Longitude E	Length (m)	Total depth (m SB)	Cored in (yr)	Recovery rate (%)
Margin	CB-01-2009	04°50.6′	36°46.8′	22	18.86	Dec 2009	81
Margin	CB-02-2010	04°48.7′	36°46.2′	10	9	Nov 2010	97
Intermediate	CB-03-2010	04°47.9′	36°47.2′	11	11	Nov 2010	98
Centre	CB-04-2010	04°43.3′	36°50.2′	10	10	Nov 2010	99.5
Centre	CB-05-2010	04°42.8′	36°51.3′	10	10	Nov 2010	97
Centre	CB-06-2010	04°44.1′	36°47.9′	10	10	Nov 2010	98.8

Table 2. I Ages from CB-01, CB-03, CB-05, and CB-06 for Chew Bahir transect chronology.

Sample ID	Core	Depth [cm]	Material	$\delta^{13}C$ [‰]	^{14}C age[b] [yr BP]	Cal. Age Range BP[c] [yr cal BP]	Area[d] [%]	WM[f] [yr cal BP]
COL 1093[a]	CB-01	153	mollusc	−1.4	1236 ± 54	1075/1192	59.3	1174
						1196/1262	40.7	
COL 1094[a]	CB-01	299	mollusc	1.7	3077 ± 54	3238/3365	97.3	3300
						3219/3230	2.7	
Beta 347311	CB-01	384–386	organic sediment	−16.0	6580 ± 60	7429/7514	88.6	7480
						7539/7561	11.4	
Beta 347312	CB-01	418–420	organic sediment	−15.6	6700 ± 60	7507/7616	100.0	7564
Beta 347313	CB-01	456–458	organic sediment	−16.6	7270 ± 80	8007/8173	100.0	8089
Beta 271307[a]	CB-01	734–735	organic sediment	−22.6	11 790 ± 120	13 446/13 795	100.0	13 629
COL 1095[a]	CB-01	976	mollusc	0.8	31 085 ± 370	35 049/36 295	100.0	35 674
COL 1096[a]	CB-01	1278	mollusc	10.1	35 508 ± 1162	39 131/41 675	100.0	40 575
COL 1097[a]	CB-01	1746	mollusc	−0.9	40 293 ± 1090	43 233/45 048	100.0	44 209
COL 1227	CB-03	126.5	mollusc fragments	−7.5	2641 ± 46	2741/2781	100.0	2758
Beta 329853	CB-03	203–204	fossillised charcoal[e]	NA	modern	NA NA	NA	0
Beta 329854	CB-03	203–204	mollusc fragments[e]	− 3.1	450 ± 60	490/530	100.0	504
Beta 347314	CB-03	210–212	organic sediment	−17.8	6930 ± 80	7675/7847	100.0	7759
Beta 347315	CB-03	256–258	organic sediment	−18.0	7770 ± 60	8509/8599	84.1	8545
						8455/8501	15.9	
Beta 347316	CB-03	344–346	organic sediment	−17.2	9360 ± 100	10 481/10 713	94.9	10 582
						10 426/10 466	5.1	
Beta 347317	CB-03	412–414	organic sediment	−16.9	10 310 ± 80	11 978/12 225	81.6	12 135
						12 257/12 381	18.4	
Beta 347318	CB-03	476–478	organic sediment	−19.5	10 060 ± 80	11 391/11 811	98.8	11 588
						11 355/11 374	1.2	
COL 1228	CB-03	509.5	mollusc	−7.2	10 079 ± 60	11 591/11 812	72.0	11 638
						11 404/11 583	28.0	
COL 1231	CB-03	521.3	mollusc[e]	−12.0	10 268 ± 82	11 821/12 154	97.9	12 028
						12 189/12 214	1.4	
						12 299/12 302	0.1	
						12 357/12 370	0.6	

Table 2. Continued.

Sample ID	Core	Depth [cm]	Material	$\delta^{13}C$ [‰]	^{14}C age[b] [yr BP]	Cal. Age Range BP[c] [yr cal BP]	Area[d] [%]	WM[f] [yr cal BP]
COL 1630	CB-03	521–522	organic sediment[e]	−24.5	11 002 ± 108	12 693/13 081	100.0	12 876
COL 1831	CB-03	712–713	mollusc fragments	−7.2	11 588 ± 148	13 276/13 645	100.0	13 443
Beta 329855	CB-03	762–764	fossilised charcoal	−25.8	1280 ± 60	1171/1288	99.0	1222
						1150/1160	1.0	
COL1234	CB-03	936–937	organic sediment	−2.9	15 647 ± 118	18 634/18 942	100.0	18 793
COL 1233	CB-03	1086–1087	organic sediment[e]	−1.7	22 155 ± 226	26 123/27 070	97.9	26 606
						27 304/27 466	2.1	
COL 1631	CB-03	1090–1091.5	organic sediment[e]	−14.4	21 939 ± 360	25 811/26 942	100.0	26 383
COL 1235	CB-05	321	mollusc fragments[e]	−10.0	10 016 ± 78	11 312/11 712	100.0	11 505
COL 1632	CB-05	321–322	organic sediment[e]	−5.7	7935 ± 90	8633/8983	100.0	8797
COL 1829	CB-05	340	mollusc	−7.8	10 138 ± 134	11 592/12 041	87.7	11 769
	CB-05					11 462/11 568	8.5	
	CB-05					11 404/11 459	3.9	
COL 1830	CB-05	405	mollusc fragments	−2.7	7015 ± 106	7722/7952	100.0	7847
COL 1633	CB-05	990–991	organic sediment	−21.8	23 921 ± 426	28 202/29 353	100.0	28 782
COL 1828	CB-06	40.5	mollusc	−0.4	213 ± 78	137/224	49.5	185
						255/316	32.4	
						0/32	15.6	
COL 1832	CB-06	233	mollusc fragments	−6.1	9994 ± 134	11 252/11 752	100.0	11 493

[a] Published in Foerster et al. (2012).
[b] Radiocarbon age with 2-sigma standard deviation.
[c] 2-sigma range of calibrated radiocarbon ages. Conventional radiocarbon ages were converted to calendar years using the IntCal09 data set (Reimer al., 2009).
[d] The relative area under the 2-sigma probability distribution.
[e] Parallel dating of biogenic carbonate and organic material and fossilized charcoal, to determine possible reservoir effect.
[f] Weighted mean of the probability density function of the calibrated age (1-sigma) as the best age estimate; using OxCal to get the probability density functions of the calibrated ages (https://c14.arch.ox.ac.uk/oxcal/). Ages in this column correspond to data shown in the age-depth model in Fig. 2.

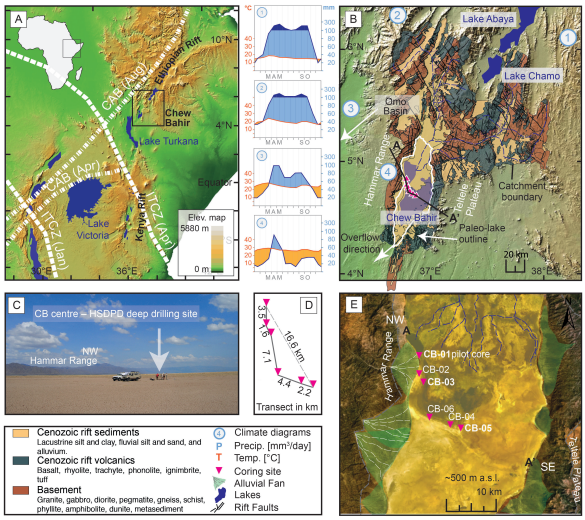

Fig. 1. Setting of the Chew Bahir site. **(A)** Chew Bahir basin within the East African Rift System with major climatic influences. Dotted lines indicate the position of the ITCZ (Intertropical Convergence Zone) and CAB (Congo Air Boundary) during different times of the year (after Tierney et al., 2011). **(B)** Map of the Chew Bahir catchment with generalized geology and rift faults within the catchment (after Davidson, 1983; Key, 1988; Hassen et al., 1991; Awoke and Hailu, 2004), major rivers, paleo-lake outline, overflow direction and sites mentioned in the text. Numbers refer to available precipitation and temperature data summarized in the climate diagrams (data: IRI, accessed October 2013). **(C)** Centre of CB basin, site of CB-05 and planned deep drilling location within the HSDPD project (2013–2014). **(D)** NW–SE transect through the Chew Bahir basin with distances between coring sites in km. **(E)** Setting of drilling location of the records discussed in this study, showing major input systems relevant for this study and position of sites within the basin.

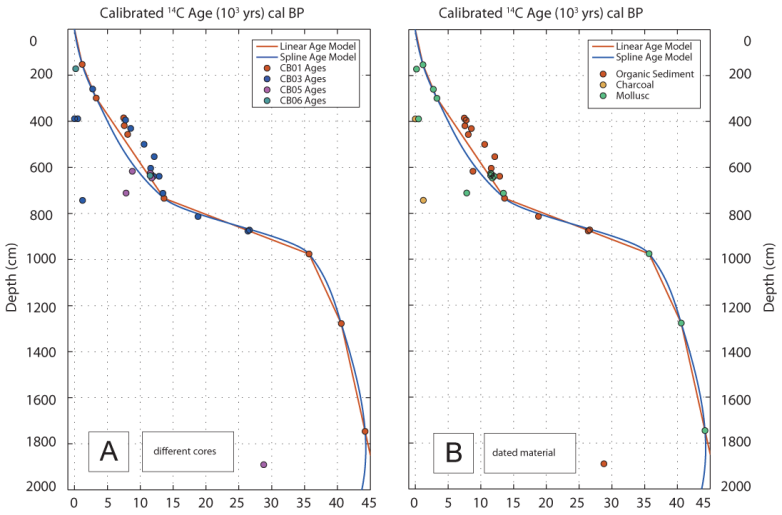

Fig. 2. Age model of tuned composite profiles of Chew Bahir cores CB01, 03–06. The depth in cm shows the composite depth of the model. Ages are the weighted mean of the probability density function and correspond to the last column in Table 2. **(A)** Radiocarbon ages per sediment core. **(B)** Materials used for radiocarbon dating.

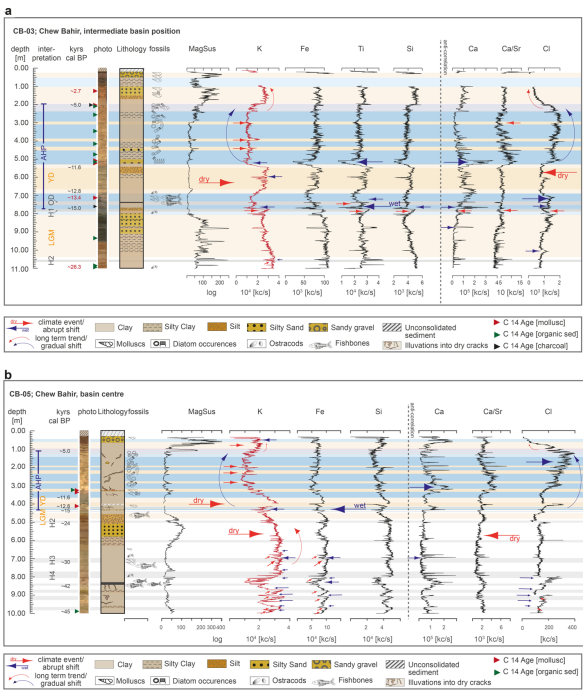

Fig. 3. Sediment composition of **(A)** CB-03 and **(B)** CB-05 with selected results of geochemical and physical analysis. Ages are given in calibrated kilo years before present. Ages in black refer to linearly interpolated values of the composite age-depth model. Red ages in **(A)** refer to radiocarbon ages from CB-03 (Table 2). Red and blue arrows point out prominent moisture shifts towards arid/humid conditions. Straight arrows indicate abrupt events, crooked show gradual trends. Orange (dry) and blue (wet) bars mark interpreted climate phases, referred to in the text; grey bars show arid phases that roughly coincide with high-latitude Heinrich events (H1–H4). MagSus – Magnetic Susceptibility; LGM – Last Glacial Maximum; YD – Younger Dryas; OD – Older Dryas; AHP – African Human Period.

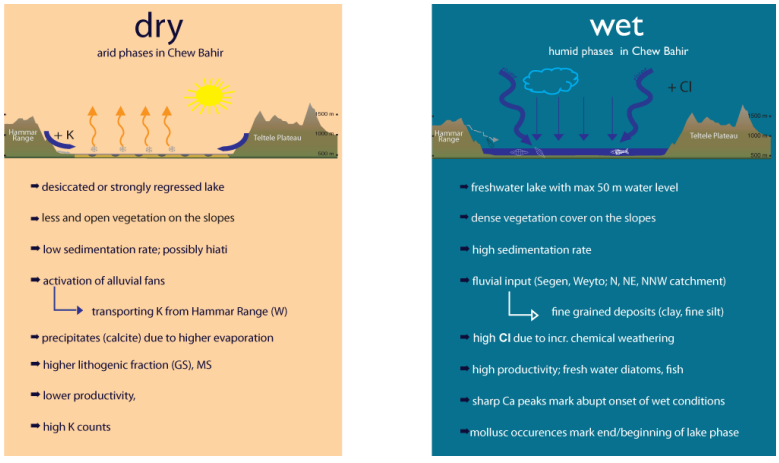

Fig. 4. Proxy evaluation for dry vs. wet conditions in Chew Bahir. These findings are highly site specific and a generalisation, an extrapolation to other sites should be handled with care and take setting of the site into consideration; exceptions can easily be found. The lake sediment proxies are controlled by three factors bound in a complex interplay: (1) distance to and restriction of the source, (2) prevailing transport mechanism (fluvial, alluvial fan activity, aeolian), that is also heavily influenced by density and type of vegetation and (3) weathering (chemical vs. mechanical).

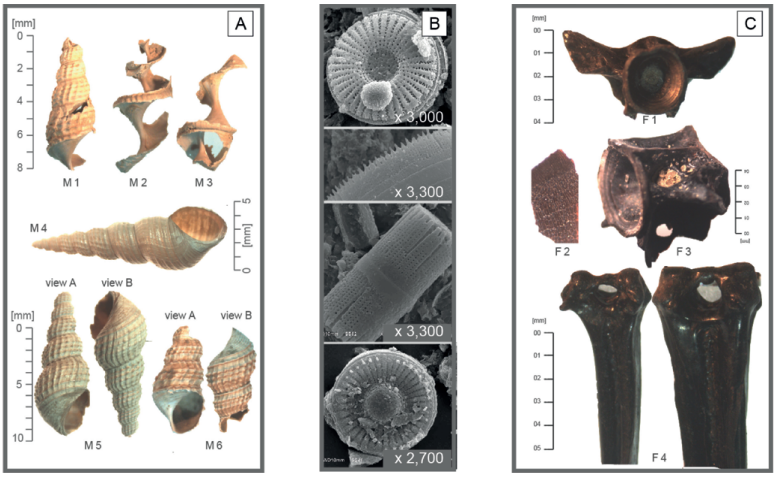

Fig. 5. Micro and macro fossils found in the Chew Bahir records CB-03 and CB-05, magnified under a binocular and a scanning electron microscope respectively. **(A)** The abundant gastropod *Melanoides tuberculata* from distinct horizon (M1–M5) in 520 cm in CB-03 and 321 cm in CB-05, both corresponding to the interval around 11–12 ka cal BP and 713 cm in CB-03, 13.5 ka cal BP (M6). **(B)** Most abundant diatoms in the assemblage from Chew Bahir (from the top): *Cyclotella*, *Aulacoseira* (detail shot of frustule end that forms long chains), *Cyclostephanos*; occurrences coincide with AHP lake phase **(C)** Fishbones, found in a distinct correlating layer in both records; 14.2 ka BP (F2), 15.2 ka BP (F1 + F4) and 32.7 ka BP (F3).

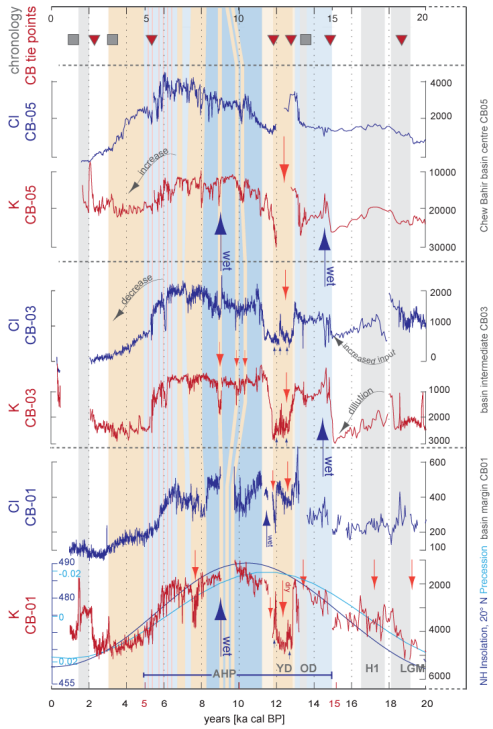

Fig. 6. The established indicators for aridity – potassium [K] – (note inverted scale) and humidity – chlorine [Cl] – show variations within the Chew Bahir basin itself. Variability comprises magnitude and proxy specific reaction towards climatic signals. Aridity proxy K reacts more sensitively towards moister increase, humidity dependent Cl^- responses sensitively to induced dry conditions. Age control along the Chew Bahir record is shown by grey squares (radiocarbon ages) and red triangles (CB correlation tie points). CB records are compared to NH summer (July) insolation variations (Laskar et al., 2004) and precession cycle (Berger and Loutre, 1991).

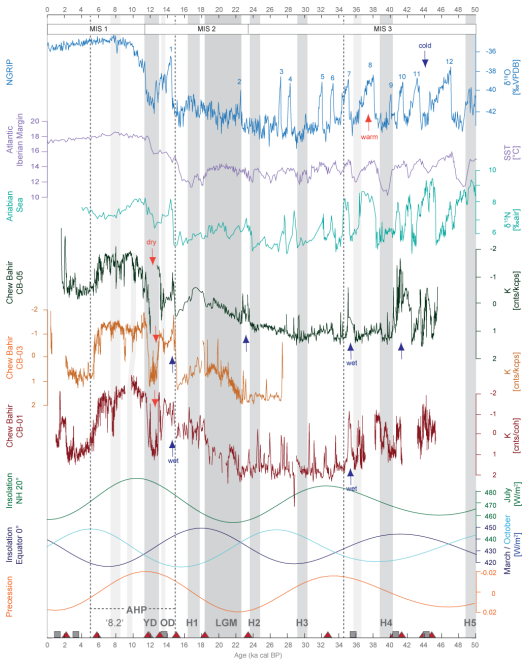

Fig. 7. Comparison of the Chew Bahir potassium (K) record with other paleo-climate records and insolation variation controlled by orbital configuration. Records plotted from top to bottom are as follows: δ^{18}O data from NGRIP (North Greenland Ice Core Project members, 2004) with numbers referring to DO-events; Alkenone derived SST reconstructions from core MD01-244 on the Iberian Margin (Martrat et al., 2007); δ^{15}N data as proxy for denitrification and productivity in the Arabian Sea in the Gulf of Oman 18° N (Altabet et al., 2002); Chew Bahir potassium (K) record from cores CB-01 (paleo-lake shore), CB-03 (intermediate), CB-05 (paleo-lake center), (note reverse scale); Insolation variations for spring and fall from the equator (Laskar, 2004); Precession cycles (Berger and Loutre, 1991). Dotted lines indicate dry–wet–dry cycle AHP. Grey bars refer to Heinrich events, Younger Dryas and H1–H5. Age control along the Chew Bahir record is shown by grey squares (radiocarbon ages) and red triangles (CB correlation tie points).